

Analyzing Inefficiencies In Veoride Bicycles

Eddie Shea¹, Ruchen Tang¹, and Sean Swalve¹

¹University of Illinois at Urbana-Champaign, Champaign, IL 61820, USA

Abstract: Non-contact infrared sensors proved useful in detecting heat inefficiencies in Veoride bicycles. The sensors were able to detect temperature changes in the foam rubber tire of the bike large enough to prove statistically significant. We quantified this heat loss using the mass and the specific heat of the tire. Although the steel chain of the bike heated up during use, the change in surface temperature was not large enough to provide a conclusive result. Attempting to quantify the heat loss in the chain also proved inconclusive.

PURPOSE

Since its invention, the bicycle has undergone numerous changes to increase its efficiency, decrease its weight, and increase its speed.¹ Countless companies still perform a balancing act between exceptional speed and efficiency and low-cost shortcuts. Veoride Inc. demonstrates this balancing act at college campuses across the United States. The company provides rental bikes at extremely low cost to their consumers. Due to their low cost, Veoride bikes must sacrifice a certain amount of speed and efficiency. The goal of this experiment is to analyze inefficiencies in Veoride bikes.

Both the chain and the tire of the Veoride pedal bike were analyzed. Data from non-contact infrared sensors produced heating and cooling curves for both the chain and the tire. The tire proved to be the main source of energy loss due to heat. The chain's heating, while not as pronounced as the tire, still demonstrated a statistically significant amount of energy loss due to heat.

THEORY

The internal energy of a system is the sum of the potential and kinetic energies of all its microscopic particles. The internal energy of a system can be increased by introduction of matter, by heat transfer, or by doing thermodynamic work on the system². Our study aims to calculate the energy loss through the chain and tire of a

Veoride bike by analyzing the temperature change of the chain and tire with respect to time. Note that all the energy loss in this case is caused by non-conservative quantities (such as friction, inelastic collisions, etc.) which eventually transform into heat. Assuming that the chain and the tire do not gain or lose any matter during the experiment---i.e., no change of the amount of matter in the chain or the tire to increase or decrease the internal energy---the change in the internal energy of the chain and tire is given by the first law of thermodynamics :

$$\Delta U = Q + W \quad (1)$$

where ΔU is the change internal energy, Q is the net heat transfer by either conduction, convection, or radiation. W is the net work done on the system by all the non-conservative quantities.

The relation between ΔU and the change in temperature, ΔT is given by:

$$\Delta U = mC\Delta T \quad (2)$$

where c is the specific heat capacity, m is the mass, and ΔT is the change in temperature. The change in specific heat of the chain and tire is negligible, since the measurement is taken in a small range of temperatures and pressures. If we assume that the chain and the tire do not wear down or pick up additional matter, the mass can

also be considered constant. Thus, relating equation (1) and a simplified version of equation (3) and rewriting in differential form:

$$\frac{\partial U}{\partial t} = \frac{\partial Q}{\partial t} + \frac{\partial W}{\partial t} = mC \frac{\partial T}{\partial t} \quad (4)$$

Specifically:

$$\frac{\partial Q}{\partial t} = P_{convection} + P_{conduction} + P_{rad\ in} + P_{rad\ out} \quad (5)$$

$$\frac{\partial Q}{\partial t} = P_{non-conservative} \quad (6)$$

where $\frac{\partial Q}{\partial t}$ is the total power of heat transfer, $P_{rad\ in}$ is the power of heat transfer through radiation into the system, $P_{rad\ out}$ is the power of heat transfer through radiation out of the system, and $P_{non-conservative}$ is the amount of work done by nonconservative quantities onto the system per unit time. Note that all of the non-conservative quantities do positive work on the system, which increases the system's internal energy.

Consider the case where a chain is thrown into an empty, radiation free vacuum space at room temperature T_0 : The power given off by radiation is given by grey body radiation:

$$P_{radiation} = \epsilon \sigma A T^4 \quad (7)$$

Where P is the total radiation power output of the object, ϵ is the emissivity constant, σ is the Stefan-Boltzmann constant ($5.67 \times 10^{-8} \frac{W}{m^2 K^4}$), A is the surface area of the grey body, and T is the temperature in Kelvin of the spherical object.

Figure 1 shows a unit of the chain. The sample chain contains 120 units.

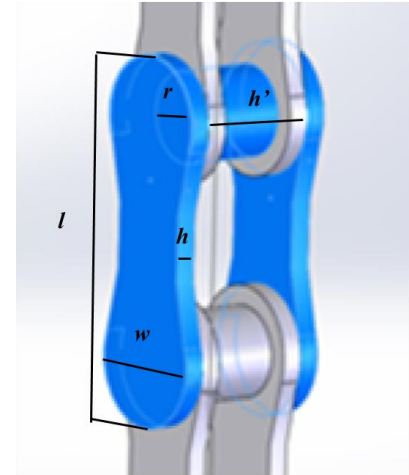


Figure 1: 3D model of a unit of the chain

We modeled the dimensions of the chain as two rectangular blocks of length $l = 0.021\ m$, width $w = 0.008\ m$, and thickness $h = 0.001\ m$. The two rectangles are attached by cylinders of radius $r = 0.0038\ m$ and height $h' = 0.0045\ m$. Thus, the surface area of a unit is approximately given by:

$$SA = 4(l \cdot w + l \cdot h + h \cdot w) + 2\pi r h' \quad (8)$$

Thus, the total area of a single chain link is $0.0009\ m^2$. The surface area of the entire chain with 120 links is thus $0.108\ m^2$. The emissivity of steel is 0.26 .³ Using these values in Equation 7 at $300\ K$, we find the power emitted by radiation is $1.43 \times 10^{-6}\ W$. $300\ K$ is the highest temperature the chain heated up to in the experiment. If the chain has this maximum temperature and is only subject to cooling by radiation:

$$\frac{P \cdot t}{m \cdot C} = 1.24 \times 10^{-5}\ K \quad (9)$$

Given that the material is carbon steel with specific heat¹⁰ $0.49 \frac{kJ}{kg \cdot K}$, the mass of the chain $m = 0.393\ kg$ and experiment cooling time $t = 30\ min = 1800s$, the maximum effect of radiation on the temperature is $1.3 \times 10^{-5}\ K$, which is negligible compared to

cooling on the order $2K$ during the 30 minute period of the experiment.

The tire can be modeled as a thin, solid hoop of inner radius 0.285 m , outer radius of 0.318 m and height 0.0375 m . The surface area is indicated by the blue colored selected part in Fig 2.



Figure 2: 3D model of a mountain bike tire

The surface area of the tire is:

$$SA = 2(R - r) + 2Rh \quad (10)$$

We used a small piece of broken tire from Veoride to estimate the mass and surface area of a whole tire by extrapolation. We used a balancing scale to find the mass of the small piece. We measured the mass of the small piece of tire as 71.2 g . We then measured the volume of the piece by assuming it was a cylinder. We measured the radius of the tire as 1.75 cm and the length of the tire as 17.2 cm . Using these measurements, we estimated the volume of the small piece of tire as $1.65 \times 10^{-4}\text{ m}^3$. Using this volume and the measured masses, we estimated the density of the foam tire as $430\frac{\text{kg}}{\text{m}^3}$. We then estimated the surface area of the tire to be 0.2 m^2 . We estimated the mass of the tire as 0.853 kg by multiplying the estimated volume by the estimated

density. The specific heat of foam rubber is $2.01\frac{\text{kJ}}{\text{kg}\cdot\text{K}}$.¹⁰ The emissivity constant for foam rubber is 0.90^2 . The maximum tire temperature we measured was 315 K . Using these values within Equation 7 we find the power emitted by the tire due to grey body radiation as 0.1 W . We neglect any incoming radiation for this power calculation.

Using Equation 9 again, we find the change in temperature due to the radiated power as 0.105 K , which is negligible compared to the accuracy of the infrared sensors ($\pm 0.5^\circ\text{C}$). The temperature change for the tire due to radiation is also negligible.

Before our team started pedaling, the temperature of chain and the tire observed by the four infrared sensors were 21.05°C , 21.39°C , 21.01°C , and 21.29°C respectively, and the ambient temperature measured by different sensor was 21.19°C . The chain can be considered at the same temperature as the environment in this case, so, the chain is in a thermal equilibrium such that the convection and conduction effects are steady. The equilibrium is given by the equation:

$$P_{rad\ in} = P_{rad\ out} \quad (11)$$

As the temperature of the chain rises, $P_{rad\ out}$ increases. However, the net effect is given by:

$$P_{net} = P_{rad\ out} - P_{rad\ in} \quad (12)$$

P_{net} will never be greater than $P_{rad\ out}$, which is the maximum possible radiation power calculated before. So, we will only focus on convection and conduction.

Although the tire was in contact with the ground, we let the bike sit on the ground 20 minutes prior to taking measurements. Thus, the tire and ground were in thermal equilibrium prior to taking measurements

and we can neglect any change in temperature coming from the ground.

SENSORS AND SETUP

The key component of our experimental setup was the Arduino Mega 2560 microcontroller. The Arduino allowed us to collect data from a number of different sensors. The most important sensor we used was the MLX90614 Digital Infrared sensor made by Melexis Technologies.

We used the MLX for two different purposes: first, to measure the surface temperature of the chain and tire. Second, to measure the ambient temperature of the air surrounding it. The highest accuracy of the sensor is $\pm 0.5^{\circ}\text{C}$ and the lowest is $\pm 4^{\circ}\text{C}$. Locally, it can safely measure temperatures from -40°C to 85°C . Remotely, it can safely measure temperatures from -40°C to 385°C . The sensor can measure surface temperature data from an angle of incidence from -90 degrees to 90 degrees, although the signal drops to 50% outside an angle of ± 45 degrees (see Figure 2).⁴

We used an Adafruit Precision Real Time Clock to keep track of time while we took our measurements. The RTC is able to read out Unix Time. Unix time is defined as the number of seconds since 00:00:00 Thursday, 1 January 1970. The RTC requires a 3V lithium coin cell battery to operate properly.⁵

We also used an Adafruit MicroSD Breakout board+ to record our measurements. The MicroSD Breakout Board compiles all of our measurements into a single text file. We then parsed through the text file to analyze our measurements.

The Ultimate GPS Breakout Board allows us to track the position of the bike while we ride it. The GPS can track up to 22 satellites at a time and updates at a frequency of 10 Hz. It has a position accuracy of < 3 meters. We also use the GPS to keep track of the bike velocity by

tracking the distance the bike traveled in a time interval of 2 seconds. The GPS also uses a 3V lithium coin cell battery as a backup in case the Arduino loses power.⁶



Figure 3: MicroSD, keypad, accelerometer, LCD, GPS, multiplexer, and BME 680 on the front of the PCB

The BME 680 Temperature, Pressure, and Humidity sensor allows us to track the ambient temperature of the air around the bike while recording our measurements. The BME can measure temperature with an accuracy of $\pm 1^{\circ}\text{C}$.⁷

The LSM9DS1 Accelerometer allows us to record the acceleration of the bike. It has $\pm 2/\pm 4/\pm 8/\pm 16$ g ranges. It also has an accelerometer offset accuracy of ± 60 mg.⁷

The Adafruit Anemometer Wind Speed Sensor allowed us to track the wind speed when we rode the bike outside. The analog sensor outputs a voltage ranging from 0.4 V to 2.0 V and can measure wind

speeds of up to 32.4 m/s.⁸



Figure 4: Battery pack, Arduino, and RTC mounted on the PCB

Finally, the I2C Multiplexer allows us to take measurements from multiple sensors with the same I2C address at the same time. This breakout board was crucial for taking infrared sensor measurements from 7 different infrared sensors. The MLX infrared sensors all have the same I2C address, and thus cannot be used at the same time on the same microcontroller. The I2C multiplexer shuttles commands between each of the sensor addresses sequentially.

As mentioned above, the infrared sensors communicate to the Arduino via I2C communication protocol. The I2C protocol allows a “master” (Arduino Mega 2560 microcontroller) to communicate with multiple “slave” integrated circuits (e.g. infrared sensors, BME 680, etc.). The I2C protocol only requires two signal lines, one SDA and one SCL. The SCL is the clock signal and SDA is the data signal. The “master” generates a start condition over the SCL lines which lets the “slave” devices know that a transmission is about to start. Then, the “master” lets its sensors know whether they will be reading or writing data. Then the data transmission starts between

the “slave” and the “master” over the SDA line. Finally, once all the data frames have been sent, the “master” will generate a stop condition.¹¹

We used a 16 x 2 Liquid Crystal Display to read out data from the Arduino and a 3 x 4 keypad to input functions into the Arduino. Figures 3 and 4 show the layout of the sensors on a custom-made printed circuit board.

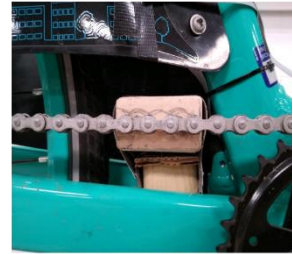


Figure 5.0: Location of the two infrared sensors pointed at the chain

Note that the infrared sensors are not attached to the circuit board. We used ribbon cables that ran into the Adafruit I2C Multiplexer to attach 6 separate infrared sensors to the Veoride bike. We 3D-printed a specialized case to attach infrared sensors

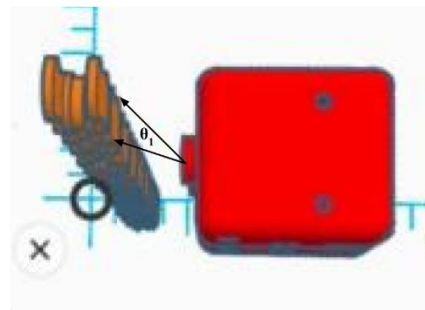


Figure 5.1: Infrared Sensor Geometry

on the chain. Figure 5.0 shows the two infrared sensors pointed at the moving chain. Note that the chain moved up and down while riding the bike. When we held the chain in place, the chain was located slightly above the two infrared sensors.

Figure 5.0 also shows this displacement. The chain was also located 4.6 ± 0.1 mm from the head of the right sensor and 5.4 ± 0.1 mm from the head of the left sensor (again refer to Figure 5.0). The top of the chain was 7.4 ± 0.1 mm from the center of the right sensor and the bottom of the chain was 2.5 ± 0.1 mm from the center of the right sensor (IR1). The top of the chain was 7.3 ± 0.1 mm from the center of the left sensor and the bottom of the chain was 2.3 ± 0.1 mm from the center of the left sensor (IR2). Using these values, calculated the angle θ_1 to be 86.66° . We calculated the angle θ_2 to be 87.93° . See Figure 5.1 for the definition of θ . Therefore, the two infrared sensors were accurately measuring 50% of the infrared signal coming from the chain (see Figure 5.2).

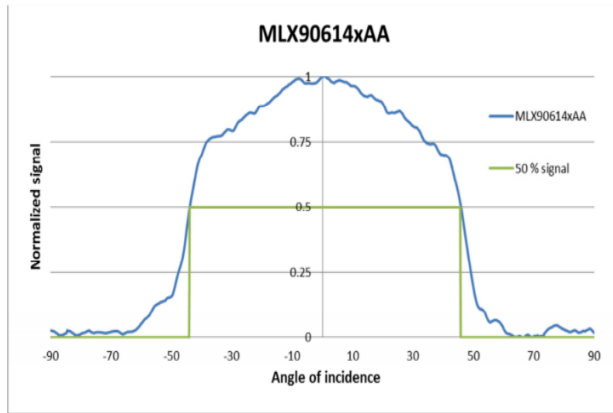


Figure 5.2: Infrared Sensor Signal Power

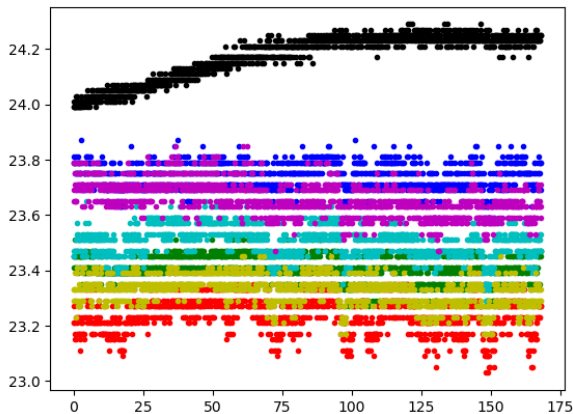


Figure 5.3: Plot of a static temperature test of the MLX90614 sensors pointing at a wall equidistant. Chain IR1 (green), Chain IR2 (blue), Tire IR1 (red), Tire IR2 (cyan), Control Tire IR (purple), Control Chain IR (yellow), and Ambient Sensor (black)

We placed all 6 infrared sensors the same distance from a wall and recorded the temperature coming from each sensor. Figure 5.3 shows the temperature coming from each sensor. From the figure, the two sensors located on the tire measured about 1.5°C higher temperatures than the control and the chain sensors. The standard deviation of our equations for differential temperature were analyzed in python using the statistics model and found the temperature variance and standard deviation to be:

$$\begin{aligned} \text{Var}(T_{Chain\ Difference}) &= 2.508 \times 10^{-3} K \\ \text{Var}(T_{Tire\ Difference}) &= 3.599 \times 10^{-3} K \\ \text{Std}(T_{Chain\ Difference}) &= 4.980 \times 10^{-2} K \\ \text{Std}(T_{Tire\ Difference}) &= 5.999 \times 10^{-2} K \end{aligned}$$

On the minimum chain scale of 1 K temperature difference, this standard deviation of 0.05 K may affect results, but the 0.06 K standard deviation for the tire sensors should not affect results of 5 and 14 K temperature differences.

We 3D printed a specialized case to attach two infrared sensors to the back tire of the bike. Figure 6 shows the two infrared sensors pointed towards the tire. We attached a broken piece of chain to the side of the bike to use as a control and pointed another infrared sensor to that. Figure 7 shows the infrared sensor pointed at the control chain. Finally, we attached a spare piece of tire to the handlebar of the bike and pointed another infrared sensor at this control tire. Figure 8 shows the infrared sensor pointed at the control tire.



Figure 6: The two infrared sensors pointed towards the back tire of the Veoride

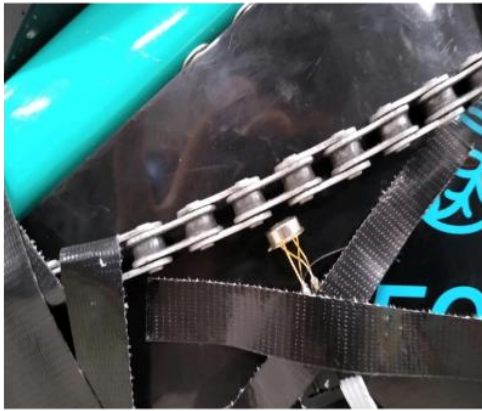


Figure 7: The infrared sensor pointed towards the control chain



Figure 8: The infrared sensor pointed towards the control tire

We connected all 6 infrared sensors to the printed circuit board located in the front basket of the bike via ribbon cable. Figure 9 shows the printed circuit board in the basket via ribbon cables.



Figure 9: Printed circuit board and wind anemometer in the basket of the bike.

We used three simple keypad inputs to operate the printed circuit board. “*00*” opened a new file on the microSD card. “*11*” told the Arduino to start taking measurements from each sensor 8 times per second. “*22*” closed the file we were writing measurements to, ensuring the file was saved on the microSD card. When reading data to the file, we measured readings from each sensor 8 times per second. When we analyzed our measurements, we averaged each sensor reading over a second and reported the averaged value at each second.

PROCEDURE

Two different experiments were conducted to determine the heating of the two main bike components associated with energy loss; one on the chain and one on the wheel. We did not include air resistance because it was too difficult to analyze for this team.⁹ Infrared temperature data were taken for all six sensors during an active riding time of 10-15 minutes and then during a cooling time of 20-30 minutes. One set of these measurements was conducted indoors on a constructed cycling roller with consistent tire friction but no wind resistance, so environmental temperature and airflow were held constant to isolate

variables that could alter the temperature. The other set was conducted outdoors in an attempt to more closely simulate the effect of variable friction and more frequent intermittent cooling (stopping) on total energy loss.

The bike would be mounted inside or placed with both tires on the riding surface for 20 minutes to reach equilibrium environmental temperature. The measuring program would be started up, ready to write data to an SD card as shown in Figures 10 and 11. The rider would attempt to ride at a fairly constant tire rotation rate (Figures 12 and 13), with some variation for outdoor measurements, for 15 minutes while the wheel and chain heated up as each rider attempted to pedal continuously at a consistent speed. The rider would then set the bike up standing still with the chain manipulated to stay taut so the sensors would be able to measure it continually cooling (Figure 14). The cooling would be conducted over 20-30 minutes so as to let both components equilibrate with the two controls. The measuring program would then be stopped and shut down and the data saved to the SD card (Figure 11). The data, saved in the form of a .txt file, was then read into python. Tools from the numpy, scipy, and matplotlib libraries were used to read, graph, clean, and analyze the data. To analyze the data, we parsed through the .txt file and separated each of the sensor values into separate arrays. We then made scatter plots of the temperature data.



Figure 10: Printed circuit board on the “Input Command” screen



Figure 11: Printed circuit board recording data



Figure 12: Riding the bike outside with the experimental setup



Figure 13: Riding the bike inside on the rollers with the experimental setup



Figure 14: The bike in a stationary position



Figure 15: Closing the file and ending the data observations

resulted in the chain temperature measurements with the least variance and tire temperature measurements with median variance. The outdoor measurement we modeled was the one with the least periodic dips due to stopping for traffic lights, and less than $1 \frac{m}{s}$ of wind speed measured when the bike was standing still.

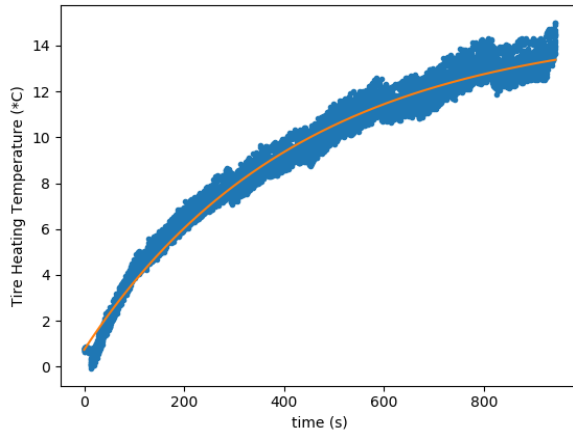
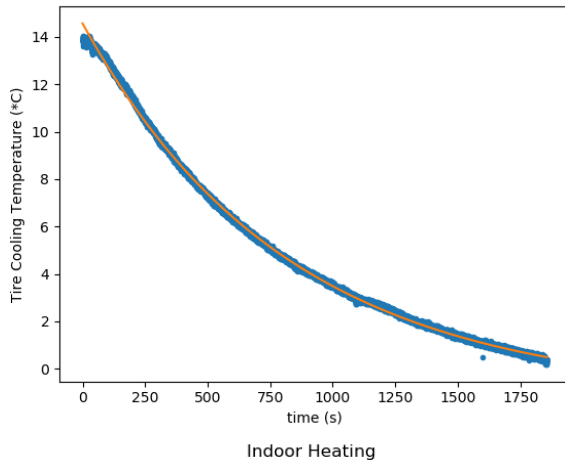
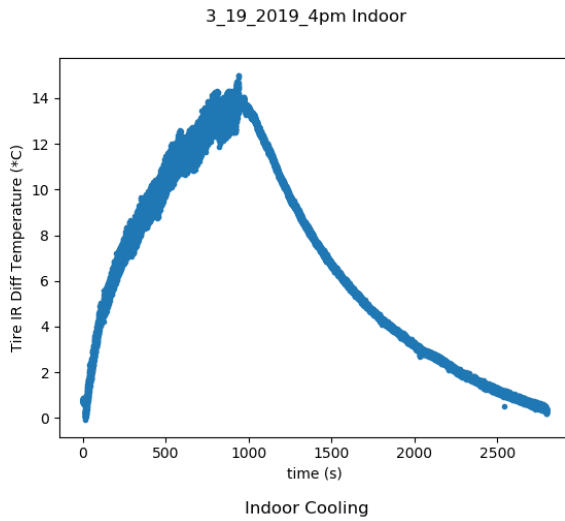
Following procedure of the indoor measurement detailed in the last section, we first analyze the indoor tire temperature data. The averaged differential IR temperature of the tire is given in Equation 13 and graphed in Figures 16:

$$\frac{(T_{Tire1} + T_{Tire2})}{2} - T_{Control} \quad (13)$$

Tire1 and *Tire2* are the first and second IR sensor temperatures read from pointing at the rear tire, and *Control* is the IR temperature read from an isolated Veoride tire fragment used as a control.

RESULTS AND ANALYSIS

The indoor measurement that was modeled was the one with the most consistent riding speed throughout, which



Figures 16: The averaged differential temperature of the tire during the indoor measurements. The first graph shows the full recording of differential temperature, while the other two show the isolated heating and cooling portions respectively. Note that the cooling curve begins at $t = 1000$ on the combined graph.

The indoor heating portion seems to include much more variance than the cooling portion. This likely has some relation to the bike moving due to the MLX90614's temperature dependence on distance from the object being measured⁴, but no specific tests were to confirm this. The Heating and the Cooling data are fitted with Equations 9 and 10 respectively.

$$T = T_{max} - (T_{max} - T_c)e^{-kt} \quad (14)$$

$$T_{max} = 14.957, T_c = 0.745, k = 2.329 \times 10^{-3}$$

$$T = T_c + (T_{max} - T_c)e^{-kt} \quad (15)$$

$$T_{max} = 14.569, T_c = -1.133, k = 1.224 \times 10^{-3}$$

These equations describe well what is shown in Figures 17; that the heating takes much less time to occur than the cooling due to a larger k factor. The mass of two tires was then calculated as 1.706 kg . The heat capacity was given by an engineering database¹⁰ as $2.01 \frac{\text{kJ}}{\text{kg} \cdot \text{K}}$. From Equation 3 we can see the power lost in the tires will be equal to:

$$P_{tot} = \frac{mC}{t_{heat}} \int_0^{t_{heat}} T dt + \frac{mC}{t_{cool}} \int_0^{t_{cool}} T dt \quad (16)$$

In this specific measurement, the total power lost is calculated using this Equation 16, and the energy lost is then calculated by dropping the total time divisor.

$$\frac{mC}{943} \int_0^{943} T_{max} - (T_{max} - T_c)e^{-kt} dt$$

$$+ \frac{mC}{1856} \int_0^{1856} T_c + (T_{max} - T_c)e^{-kt} dt$$

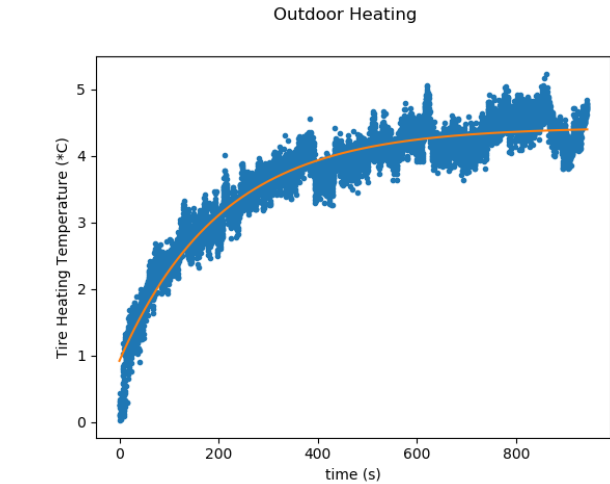
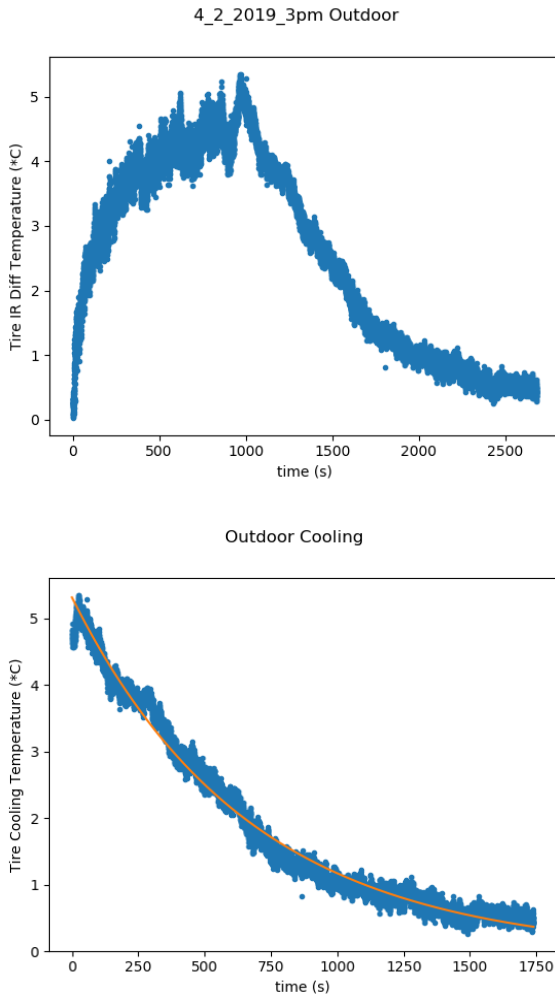
$$P_{tot} = (8680.945 + 9402.559) \cdot$$

$$\left(\frac{1.706 \cdot 2.01}{2799} \right) \cdot \left(K \cdot s \cdot kg \cdot \frac{\text{kJ}}{\text{kg} \cdot \text{K}} \cdot \frac{1}{s} \right)$$

$$P_{tot} = 22.154 \text{ W} \rightarrow U_{tot} = 62.009 \text{ kJ}$$

This is a fairly large amount of power being lost in the tire, but perhaps this larger magnitude with the same total temperature variance within the sensors is why the temperature graphs for the tires appear to be much smoother and well defined than those of the chains.

Following procedure of the outdoor measurement detailed in the last section, we now analyze the outdoor tire temperature data. The averaged differential IR temperature is the same Equation 13 and its graphs are shown in Figures 17



Figures 17: The averaged differential temperature of the tire outside. The first graph shows the full recording of differential temperature, while the other two show the isolated heating and cooling portions respectively. Note that the cooling curve starts at $t = 1000$ on the combined graph.

The outdoor heating and cooling portions seem to include more variance than the indoor measurements, with a far lower maximum temperature difference. The larger variance could be a factor of more movement occurring, or more airflow for convective cooling, but data is lacking to thoroughly conclude either cause. The lower maximum temperature difference for the tires could also be a factor of more wind for convective cooling or contact cooling with the road that wouldn't occur on a roller. The heating and the cooling are fitted with the same equations 10 and 11 with constants listed here.

$$T = T_{max} - (T_{max} - T_c)e^{-kt}$$

$$T_{max} = 4.483, T_c = 0.961, k = 4.627 \times 10^{-3}$$

$$T = T_c + (T_{max} - T_c)e^{-kt}$$

$$T_{max} = 5.192, T_c = 1.409, k = 1.547 \times 10^{-3}$$

Once again, the heating occurs much more quickly than the cooling, and since we are still observing the tires, the constants for mass and heat capacity will be the same. It then follows the integration for total will be the same Equation 16 with different time

bounds. In this measurement, the total power lost is calculated as:

$$\frac{mC}{969} \int_0^{969} T_{max} - (T_{max} - T_c)e^{-kt} dt + \frac{mC}{1714} \int_0^{1714} T_c + (T_{max} - T_c)e^{-kt} dt$$

$$P_{tot} = (3591.439 + 4687.904) \cdot \left(\frac{1.706 \cdot 2.01}{2683} \right) \cdot \left(K \cdot s \cdot kg \cdot \frac{kJ}{kg \cdot K} \cdot \frac{1}{s} \right)$$

$$P_{tot} = 11.042 W \rightarrow U_{tot} = 29.624 kJ$$

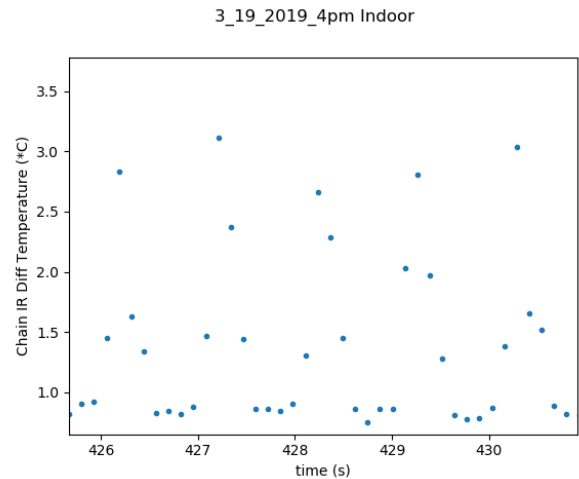
This seems to be only 49.8% the power lost within the tires riding outside compared to the indoor observation. But, to fully explain this discrepancy, we need to compare the power lost in the chain and the expected total power use in each

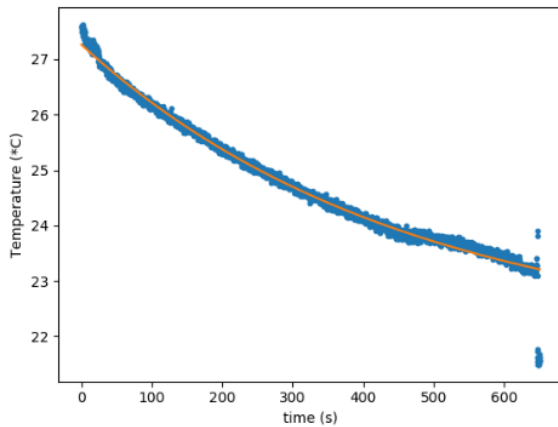
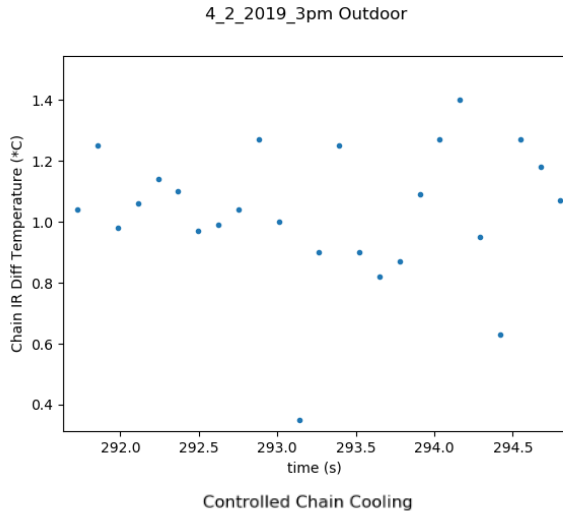
Following procedure detailed in the last section, the averaged differential IR temperature of the chain is a modified version of Equation 13:

$$\frac{(T_{Chain1} + T_{Chain2})}{2} - T_{Control} \quad (17)$$

Chain1 and Chain 2 are the first and second IR sensor temperatures read from pointing at the chain with slight distance variation, and Control is the IR temperature read from an isolated Veoride chain fragment used as a control. Only the indoor measurement was able to be modeled in python because the fitting algorithm couldn't model a fit that converged to a r^2 value greater than 0.5 for both the heating and cooling curves. This inconsistency of the measurement data is possibly due to the chain's quicker cooling in the air with non-zero wind speed or much lower heat capacity, not allowing an effect of less than 1W to emerge as statistically in the data.

Two questions stem from the chain heating/cooling graph; why was the heating portion so varied? And are we sure the chain was actually cooling? When looking at only a few data points of heating, we realized the heating variation was very periodic. We thought that could be the chain moving in view, but that would occur twice a second with $\approx 60 rpm$ pedaling. It was then experimentally determined that the cause of the heating was the rider's leg coming into view. For this reason, in heating analysis, we decided to truncate the temperature values above the maximum value of just the chain. The frequency measurement was conducted on the outdoor measurements well. We also heated the chain in a controlled manner to confirm that it cooled along a curve and with roughly the same rate as in experimentation. These three tests confirmed suspicions and are shown in Figures 18.





Figures 18. An example of the periodic increase and decrease of chain temperature every second due to the rider's leg coming into the sensor image area on the top. On the bottom is the cooling of the chain after being heated in a controlled manner.

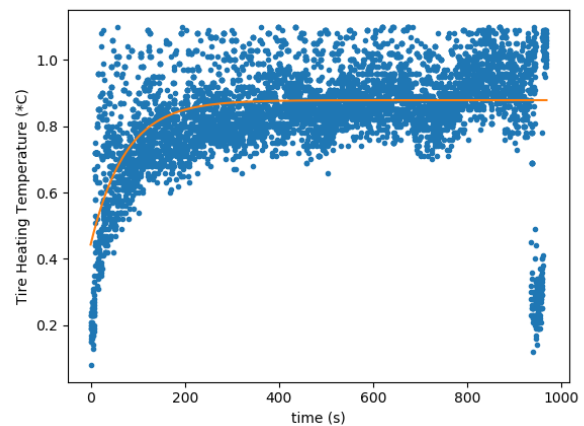
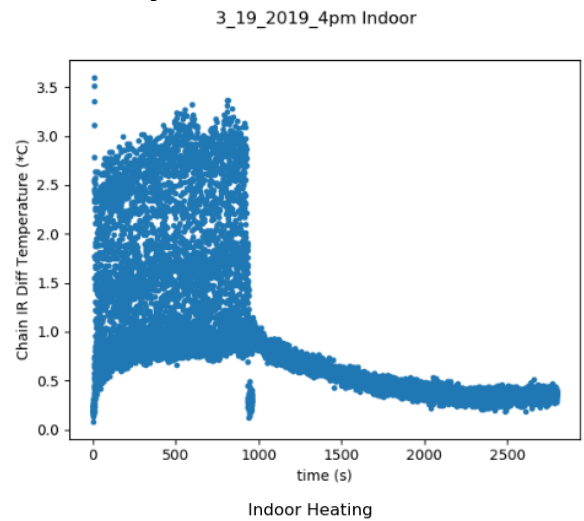
Even though the temperature data was not analyzable, we were able to extrapolate the mean speed of the bicycle in the outdoor tests. Using the gear ratios of the Veoride and the frequency of the outdoor beats shown in Figure 17, we can calculate the relative speed of the bicycle in the outdoor tests as

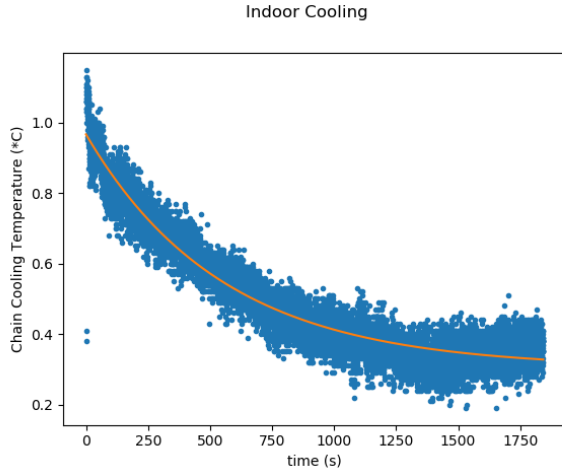
$$1.859 \frac{rev}{s} \cdot 1.833 \cdot 1.360 \cdot 1.0m = 4.634 \frac{m}{s}$$

The Martin Milliken study calculated an average continuous power input for $11 \frac{m}{s}$ on a flat plane with negligible wind as $225 W$.

A ride with an average $4.634 \frac{m}{s}$ speed with less than 2 m of height change should have a power use of $94.778 W$. Thus, the tires use 11.650% of the total expected power output. This figure is within the $10\text{-}20\%$ range the Martin Milliken study found for air filled tire bikes.

We also attempted to analyze that measurement shown in Figures 19 in the same way as the tires with this new knowledge of the leg causing quick periodic temperature change, and confirmation the chain actually cooled.





Figures 19. The averaged differential temperature of the chain indoors with heating and cooling separated and heating controlled for the IR detection of the rider's leg. Note that the cooling curve starts at $t = 1000$ on the combined graph.

Applying the same heating and cooling equations as before, we can analyze directly the power loss during the indoor heating and cooling of the chain:

$$T = T_{max} - (T_{max} - T_c)e^{-kt}$$

$$T_{max} = 0.879, T_c = 0.432, k = 9.088 \times 10^{-3}$$

$$T = T_c + (T_{max} - T_c)e^{-kt}$$

$$T_{max} = 0.899, T_c = 0.267, k = 1.386 \times 10^{-3}$$

With the same integration procedure as before, with the heat capacity of a steel chain given by an engineering database¹⁰ as $0.49 \frac{kJ}{kg \cdot K}$ we find the energy loss to be:

$$\frac{mC}{943} \int_0^{943} T_{max} - (T_{max} - T_c)e^{-kt} dt$$

$$+ \frac{mC}{1856} \int_0^{1856} T_c + (T_{max} - T_c)e^{-kt} dt$$

$$P_{tot} = (779.721 + 916.725) \cdot \left(\frac{0.393 \cdot 0.49}{2799} \right) \cdot \left(K \cdot s \cdot kg \cdot \frac{kJ}{kg \cdot K} \cdot \frac{1}{s} \right)$$

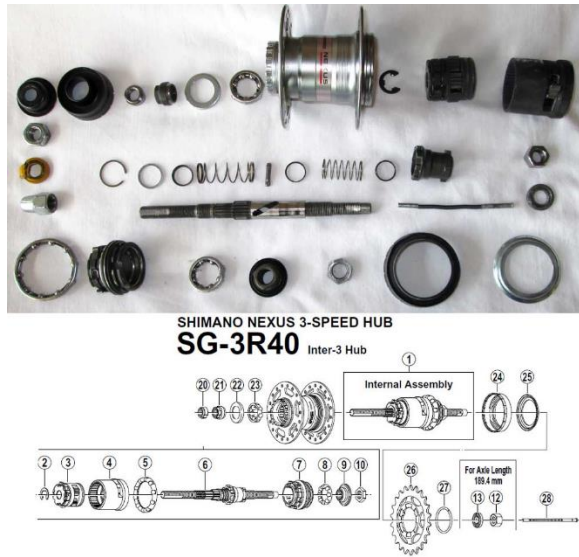
$$P_{tot} = 0.117 W \rightarrow U_{tot} = 326.685 J$$

This shows that our energy losses in the chain have a calculated value of only $326.685 J$ and $0.117 W$ of power are being

lost in the chain. This is roughly 0.5% of the energy lost in the tire. Using the gear ratios of the Veoride and the Frequency of the beats shown in Figure 17, we can calculate the relative speed of the bicycle in the indoor tests as

$$0.909 \frac{rev}{s} \cdot 1.833 \cdot 0.733 \cdot 1.0m = 1.222 \frac{m}{s}$$

A ride with a calculated average $1.222 \frac{m}{s}$ during a riding portion and $0 \frac{m}{s}$ over a cooling portion should have a power use of $24.995 W$. The energy loss of the tire at $22.154 W$ or 88.634% of total expected energy loss, and the lack of any energy expended fighting air resistance on the rollers, suggests the chain energy losses should be close to the remaining power and thus small, especially because the expected standard deviation of read temperatures would only account for a 5% error in the chain energy loss and a 0.4% error in the tire energy loss. Therefore, this $0.117 W$ measurement is about one-half the expected value⁹ and doesn't fully explain the missing energy. During our analysis on the Veoride, we could only find two possible conclusions for the missing energy; greater sensor error than in control measurements due to distance variation from vibrations and unmeasured energy loss in the gear shifter, shown in Figure 20. Both are easily possible explanations which do not undermine the validity of this study.



Figures 20. The Veoride gear shifting mechanism which was impossible to access and measure without destroying the bike.

As a final point of analysis, we can attempt to use this chain energy loss to extrapolate the missing power consumption for the outside measurement. This requires the assumption from the Martin Milliken study that chain energy losses scale roughly linearly with velocity in a low wind environment.⁹ Making this assumption and assuming the difference in environments has much greater effect on the tires than the chains, we can extrapolate the expected chain energy loss on the outside measurements as:

$$\frac{4.634}{1.222} \cdot 0.177W = 0.444W$$

Using this estimate of the chain power loss and comparing it to the measured $11.042 W$ within the tires during a real ride, we find an estimated ratio of chain to tire power loss of 1:25. This is far less than even the least efficient air-filled tire bicycles at 1:17.⁹

CONCLUSION

The energy loss within the Veoride rideshare bicycle was analyzed through the use of infrared temperature sensors, on

board time recording, and by riding in two different environments; indoors and outdoors. The focus was on the temperature difference between surface mounted fragments of a chain and tire, and their corresponding heating components on the bike. Both the indoor and outdoor measurements showed clear and substantial heating on the bike tires modeled at $11.042 W$ and $22.154 W$ of power consumed heating the tire through friction outside and inside respectively. This translated into $29.624 kJ$ and $62.009 kJ$ lost in 12-15-minute rides. The difference between these wattages do not have a conclusive cause but are likely due to higher friction between the rollers and the tires than the road.

The chain showed no significant evidence of heating in either the outdoor tests because even though the pattern of heating and cooling curves roughly emerged in two instances, neither showed fitted temperature curves that were statistically significant, but they did allow us to determine the riding speed through frequency analysis. The indoor chain measurements did allow us to analyze the chain heating in a way that should be consistent with outdoor chain energy losses given that the rolling friction of the rollers wouldn't affect the chain. Furthermore, trying to functionally model the chain heating and cooling yielded an energy loss of $36.685 J$ and $0.117 W$ of power. Extrapolating this to the outdoor case, we estimated a chain to tire energy loss ratio of 1:25, which is an even smaller ratio than the least efficient air-filled tire bicycles which have 1:17. Even though further research is needed to make more substantive conclusions about energy loss, we can currently conclude the Veoride bikes lose far more energy in heat through their tires than the chain compared to bicycles designed for efficient street riding.

REFERENCES

- [1]: Mozer, David. "Chronology of the Growth of Bicycling and the Development of Bicycle Technology." International Bicycle Fund, <http://www.ibike.org/library/history-timeline.htm>
- [2]: Bergmann, Gustav. "Natural Philosophy of Cause and Chance. Max Born." *Philosophy of Science*, vol. 17, no. 2, 1950, pp. 146–149., doi:10.1086/287082
- [3]: "Emissivity Coefficients Materials." EngineeringToolBox, www.engineeringtoolbox.com/emissivity-coefficients-d_447.html
- [4]: "MLX90614ESF-BCA-000-SP-ND." Digi-Key Electronics, <https://www.digikey.com/products/en?mpart=MLX90614ESF-BCA-000-SP&v=413>
- [5]: "Adafruit PCF8523 Real Time Clock." Adafruit Industries, <https://learn.adafruit.com/adafruit-pcf8523-real-time-clock/overview>
- [6]: "Adafruit Ultimate GPS Breakout." Adafruit Industries, <https://www.adafruit.com/product/746>
- [7]: "Adafruit BME 680 - Temperature, Pressure, Humidity, and Gas Sensor." Adafruit Industries, <https://www.adafruit.com/product/3660>
- [8]: "Anemometer Wind Speed Sensor w/ Analog Voltage Output." Adafruit Industries, <https://www.adafruit.com/product/1733>
- [9]: Martin, J. C., Milliken, D. L., Cobb, J. E., McFadden, K. L., & Coggan, A. R. (1998). Validation of a mathematical model for road cycling power. *Journal of applied biomechanics*, 14(3), 276-291.
- [10]: "Specific Heat of Solids." EngineeringToolBox, https://www.engineeringtoolbox.com/specific-heat-solids-d_154.html
- [11]: "I2C." Sparkfun, SFUPTOWNMAKER, <https://learn.sparkfun.com/tutorials/i2c/all>